

**Desalination & Water Purification Research
and Development Program Report No. XXX**

Producing Polymeric Membrane for Ultrafiltration by High Internal Phase Emulsion Templating

Prepared for Reclamation Under Agreement No. XXXXXXXXXXXXX

by

Anna Malakian and Reza Foudazi



U.S. Department of the Interior
Bureau of Reclamation
Technical Service Center
Water and Environmental Services Division
Water Treatment Engineering Research Team
Denver, Colorado

November 2015

MISSION STATEMENTS

The mission of the Department of the Interior is to protect and provide access to our Nation's natural and cultural heritage and honor our trust responsibilities to Indian tribes and our commitments to island communities.

The mission of the Bureau of Reclamation is to manage, develop, and protect water and related resources in an environmentally and economically sound manner in the interest of the American public.

Disclaimer

The views, analysis, recommendations, and conclusions in this report are those of the authors and do not represent official or unofficial policies or opinions of the United States Government, and the United States takes no position with regard to any findings, conclusions, or recommendations made. As such, mention of trade names or commercial products does not constitute their endorsement by the United States Government.

Acknowledgements

The authors would like to thank the U.S. Bureau of Reclamation and New Mexico State University for their support.

Contents

Executive Summary	1
1. Introduction	2
1.1. Water scarcity	2
1.2. Emulsions.....	3
1.3. High Internal Phase Emulsions	6
1.4. Polymerization of High Internal Phase Emulsions	8
2. Experimental.....	11
2.1. Materials	11
2.2. Emulsion preparation	11
2.3. Sample preparation	16
2.4. Characterization	19
2.4.1. Morphology.....	19
2.4.2. Surface Chemistry.....	19
2.4.3. Mechanical Properties.....	20
2.4.4. Filtration test	21
3. Results and Discussion	22
3.1. Morphology.....	22
3.2. In-situ functionalization	28
3.3. Mechanical properties	31
3.4. Permeability	32
4. Conclusion	35
5. References	36

Table of Figures

Figure 1. Schematic of different types of emulsions	4
Figure 2. Schematic of the emulsion instability processes	6
Figure 3. Schematic representation of high internal phase emulsions.....	7
Figure 4. Typical micrographs of (a) HIPE and (b) polyHIPE [20]	9
Figure 5. Structure of majorly used chemicals	11
Figure 6. Oven used to polymerize samples containing thermal initiator	16
Figure 7. UV cross-linker used to polymerize samples containing photo initiator	17
Figure 8. Schematic process of polyHIPE synthesis.	17
Figure 9. HIPE preparation setup.....	18
Figure 10. Casting thin layer of HIPE on support for membrane applications.....	18
Figure 11. Soxhlet setup for washing polyHIPES.....	19
Figure 12. conductometric titration setup	20
Figure 13. Mechanical tester equipment used to determine the resistance of membranes against pressure	21
Figure 14. Homemade filtration setup	22
Figure 15. Optical micrographs of sample #17 after A) 0 min, B) 5 min, C) 10 min, D) 30 min, and E) 60 min of mixing. The scale bar is equal to 10 μm	23
<i>Figure 16. Optical microscopy of sample #27: A) 0 min, and B) 5 min after casting on glass slide. The scale bar is equal to 10 μm.....</i>	<i>24</i>
<i>Figure 17. Comparison of (A) droplet size of HIPE before polymerization obtained by optical microscopy (scale bar: 10 μm), and (B) void size of polyHIPE after polymerization obtained by SEM (scale bar: 50μm) for sample #14.</i>	<i>25</i>
Figure 18. Droplet/void size distribution before and after polymerization (Sample #100)	25
Figure 19. Different window formation: A) SEM of sample #26: no window formation, B) SEM of sample #35: some window formation, C) SEM of sample #46: some window formation, D) SEM of sample #100: intermediate window formation in term of size and volume, E) SEM of sample #62: large window formation. The scale bar is equal to 5 μm	26

Figure 20. Pore size distribution of sample #100	27
Figure 21. Window size distribution of sample #100	27
<i>Figure 22. Schematic of in-situ functionalization process of polyHIPE developed in this work.....</i>	<i>28</i>
Figure 23. Comparing FTIR results of polyHIPE before and after washing with solvent to study the reactivity of surfactant (sample #21)	29
Figure 24. FTIR results show change in surface chemistry for polyHIPEs with (sample #47) and without sodium acrylate (sample #21)	29
Figure 25. Titration curve for: (A) DI water, (B) polyHIPE without sodium acrylate, and (C) polyHIPE with 1 wt.% sodium acrylate	30
Figure 26. Stress versus strain curve of polyHIPE with different pore volume fraction (samples #89, 90, and 91).....	32
Figure 27. Drying kinetics of polyHIPE without (sample #10), with 0.5% (sample #40), with 1% (sample #45), and with 2% (sample #50) sodium acrylate	34

Glossary

HIPE	High Internal Phase Emulsions
polyHIPE	Polymerized high Internal Phase Emulsions
EPA	Environmental Protection Agency
UF membrane	Ultrafiltration membrane
MF membrane	Microfiltration membrane
W/O	Water-in-oil emulsions
O/W	Oil-in-water emulsions
O/O	Oil-in-oil emulsions
W/W	Water-in-water emulsions
O/W/O	Oil-in-water-in-oil emulsions
W/O/W	Water-in-oil-in-water emulsions
HLB	Hydrophilic-lipophilic balance
BA	Butyl Acrylate
SA	Sodium Acrylate
Span 80	Sorbitane monooleate
PGPR	Polyglycerol polyricinoleate
DVB	Divinylbenzene
KPS	Potassium persulfate
1-HPK	1-Hydroxycyclohexyl phenyl ketone
BPO	Benzoyl Peroxide
DMT	N,N-dimethyl-p-toluidine
EGDMA	Ethylene Glycol Dimethacrylate
SEM	Scanning electron microscopy
FTIR	Fourier transform infrared spectroscopy
κ	Darcy's constant (m^2)
l	Membrane thickness (μm)
Q	Flow rate (m^3/s)
μ	Feed viscosity (Pa.s)
A	Membrane area (mm^2)
ΔP	Pressure difference along the membrane (Pa)
R	Rejection
C_p	Permeate concentration (g/L)
C_f	Feed concentration (g/L)

Executive Summary

Presently, over one-third of the world's population lives in water-stressed countries, and this figure is predicted to rise to nearly two-thirds by 2025 [1]. Demand for membrane systems and disinfection equipment will increase as the Environmental Protection Agency (EPA) implements new regulations that stipulate maximum allowable limits for disinfection byproducts, volatile organic compounds, perchlorates, and other potentially hazardous contaminants [2]. Therefore, adequate access to low-cost, energy-efficient methods for advanced water treatment, without further stressing the environment, requires designing and evaluating new membrane technologies.

In this project, high Internal Phase Emulsions (HIPEs) are used as template for producing porous polymers with high porosity and permeability [3]. Porous polymers from HIPE templating are synthesized with a highly interconnected pore network, and thus, have the potential to be utilized for producing microfiltration and ultrafiltration membranes. In this work, oil phase as continuous phase containing butyl acrylate monomer was polymerized through radical polymerization. For improving the mechanical properties, ethylene glycol dimethacrylate as a cross-linker was added to the oil phase. Polyglycerol polyricinoleate was mainly used as surfactant to stabilize HIPEs. Aqueous dispersed phase containing salt and in some formulations initiator was added drop-wise to the oil phase while mixing was performed with an overhead mixer. Different initiation systems such as redox, thermal, and photo initiator were investigated for optimum polymerization of HIPE. We found that mixtures of thermal and photo initiator provide satisfactory stability and polymerization. Then, the volume fraction, speed and time of mixing, and surfactant concentration were varied to produce different polyHIPE membranes. The membranes performance was evaluated in terms of pore size, porosity, and window formation. The optimum formulation was considered as the one with mechanical properties high enough to withstand the filtration pressure, the highest window formation (compared to other synthesized polyHIPEs in this work), and the smallest possible

pore size. Hydrophobic matrix and hydrophilic surface can result in improved rejection and permeability of porous membranes. Therefore, in-situ functionalization of polyHIPEs was investigated through incorporation of a hydrophilic monomer (sodium acrylate) in the water phase of HIPE prior to polymerization. After successful functionalization, the membrane performance was studied. The results show that polyHIPEs can successfully be used as ultrafiltration (UF) membranes in upper bond ($\sim 0.1 \mu\text{m}$) as well as microfiltration (MF) membranes, especially for removal of suspended particles. The produced polyHIPE membranes have higher permeability than typical commercial UF membranes. Therefore, they require less energy for filtration compared to current membranes in the market.

1. Introduction

1.1. Water scarcity

As the world population continues to grow, water resources become scarcer, particularly in arid and semi-arid regions. Consequently, there will be an increase in the production of wastewater containing enough harmful material to damage ground water and/or surface water quality, which should be treated to meet the environmental regulations. Small communities face unique challenges in finding wastewater management solutions since they simply lack the capacity to pay for capital improvements and costs associated with the operation and maintenance of a wastewater system. Additionally, over one-third of the world's population lives in water-stressed countries, and this figure is predicted to rise to nearly two-thirds by 2025 [1].

Demand for membrane systems and disinfection equipment will increase as the Environmental Protection Agency (EPA) implements new regulations that stipulate maximum allowable limits for disinfection byproducts, volatile organic compounds, perchlorates, and other potentially hazardous contaminants [2]. Therefore, adequate access to low-cost, energy-efficient methods for advanced water treatment, without further stressing the environment, requires designing and

evaluating new membrane technologies. In this project, the high internal phase emulsions templating is used to produce new generation of ultrafiltration and microfiltration membranes. The aim is to develop membranes through ecofriendly process, while increasing their permeability in order to reduce the cost of water treatment.

1.2. Emulsions

An emulsion is a dispersion of one liquid (the dispersed or internal phase) in a second immiscible liquid (the continuous or external phase). Emulsions are part of a more general class of two-phase systems of matter called colloids. Examples of emulsions include butter, margarine, mayonnaise, and cream. As schematically shown in Figure 1, emulsions are classified based on the dispersion of droplets in continues phase. The system which consists of water droplets dispersed in an oil phase is known as a water-in-oil (w/o) emulsion, while the dispersed oil droplets in an aqueous phase is an oil-in-water (o/w) emulsion. Additionally, there are more complicated cases such as oil-in-water-in-oil (o/w/o) and water-in-oil-in-water (w/o/w) emulsions, known as multiple emulsions.

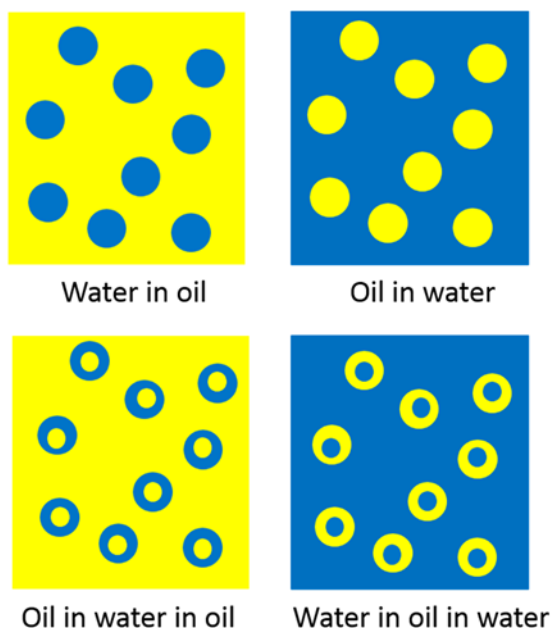


Figure 1. Schematic of different types of emulsions

Beside the oil and water phases, emulsions contain surfactant that stabilizes the dispersed droplets. In other word, while emulsions are not thermodynamically stable systems, they can kinetically be stabilized over a period of time by using proper surfactants. The molecular structure of surfactants contains two moieties: one has attraction for water, known as a lyophobic (hydrophilic) part or “head”, while the other part has strong attraction for oil, called the lyophilic (hydrophobic) segment or simply “tail”. Such molecular structure is known as amphipathic or amphiphilic. In the case of a surfactant dissolved in aqueous medium, the lyophobic (hydrophobic) group distorts the structure of the water by breaking hydrogen bonds between the water molecules and by structuring the water in the vicinity of the hydrophobic group [4]. Therefore, the free energy increases, and the system responds in some fashion to minimize the contact between the lyophobic group and the water phase. Formation of micelles by surfactant molecules is a result of such tendency.

Based on the first emulsification rule developed by Bancroft in 1913 [5], surfactants improve the dispersion of the phase in which they do not dissolve very well. Surfactant can be classified by their hydrophilic-lipophilic balance (HLB) which for first time was introduced by Griffin [6] in 1946. One of the popular formula for calculation of HLB is the Davies expression [7]:

$$HLB = 7 + (\text{Hydrophilic group number}) - 0.45 n_c$$

where hydrophilic group number is obtained form group contribution theory and n_c is the number of $-\text{CH}_2-$ groups in the lipophilic part of the molecule. Surfactants with an HLB number in the range of 3 to 6 form water-in-oil (w/o) emulsions, whereas those with HLB numbers of 8 to 18 are expected to form oil-in-water (o/w) emulsions. Surfactants should be insoluble in the droplet phase to prevent emulsion inversion at high internal phase volume fractions. Depending on the nature of the hydrophilic head group, surfactants are classified as ionic (anionic, cationic, zwitterionic) which have a charged head group connected to a neutral tail, or nonionic which have an uncharged, polar head group connected to

a hydrocarbon tail. As mentioned above, surfactants play a major role in the preparation and stabilization of emulsions. They can be adsorbed strongly at the interface between the continuous and dispersed phases and reduce the energetic driving force to coalescence by lowering the interfacial tension and/or forming a mechanical barrier between droplets.

The interfacial chemistry and rheology, the dynamic of adsorption, and the physicochemical kinetics of surfactants are important parameters in emulsion stability [2]. There are two principal types of stability for colloidal emulsions, droplet stability and dispersion stability. Droplet stability is dependent on the bulk properties of the fluids and the nature of the surfactant. Several breakdown processes may occur that depend on the particle size distribution and the density difference between droplets and the medium. However, the physical phenomena involved in each instability process are not simply described, requiring analysis of the various forces involved [8]. Generally, the solubility of the dispersed droplets and the particle size distribution determine Ostwald ripening and the stability of the liquid film between the droplets determines coalescence and phase inversion. Ostwald ripening is a process where large drops grow at the expense of smaller ones, as the larger droplets are energetically more favorable. Dispersion stability is the stability against aggregation, flocculation (coagulation), and macroscopic phase separation [9]. Emulsion droplets come into contact with each other due to Brownian motion. Consequently, coagulation (flocculation) can occur, which may lead to the formation of larger droplets and coalescence. By forming a thin film around the dispersed phase, as mentioned previously, the surfactant provides a barrier against coalescence and lowers the interfacial tension of the system. A continuous phase with high viscosity can reduce creaming and flocculation by impeding Brownian motion. However, an increase in the viscosity of the continuous phase can lead to inefficient mixing of the two phases [10]. Figure 2 (adapted from ref. [8]) schematically shows different instability in emulsion systems.

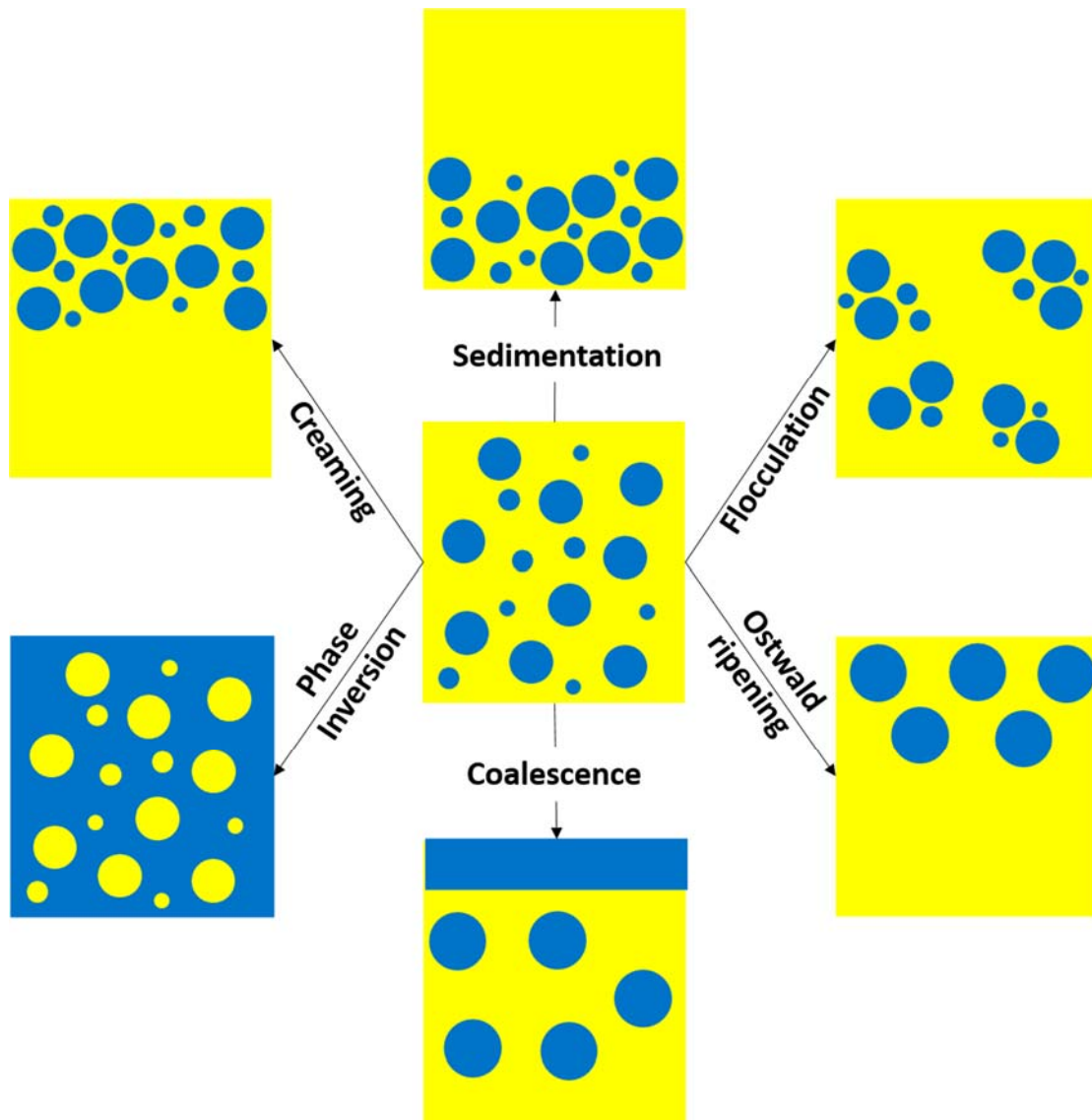
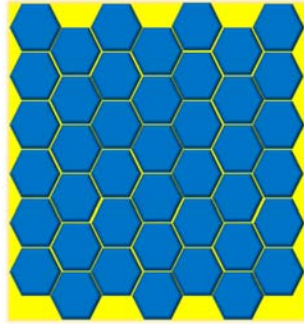


Figure 2. Schematic of the emulsion instability processes

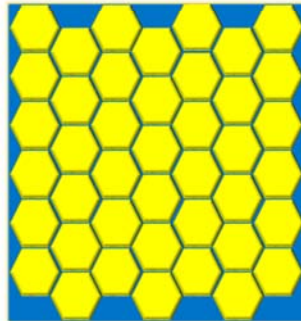
1.3. High Internal Phase Emulsions

The shape of droplets in dispersed phase is spherical (minimum surface area in constant volume) as schematically shown in Figure 1. The volume fraction of maximum closest packing of monodispersed spheres is 74.01% [11]. If the concentration of dispersed phase exceeds this fraction, droplets will be deformed into polyhedrons. This deformation will create large areas of contact between droplets and a packed configuration which induces mechanical interference between droplets, thus prohibiting their free movement (Figure 3). Such emulsions are known as “high internal phase emulsions” (HIPES) or “highly

concentrated emulsions” (HCEs), as introduced by Lissant [12] for the first time in 1964.



High internal phase emulsion (water-in-oil)



High internal phase emulsion (oil-in-water)

Figure 3. Schematic representation of high internal phase emulsions

HIPES similar to other emulsions are thermodynamically unstable and may go through instability. Coalescence in HIPE can occur through the rupture of thin films between the adjacent droplets, eventually leading to complete phase separation of the HIPE. Creaming/sedimentation is the formation of a concentrated layer above/below the bulk emulsion, due to density differences between the two phases.

One of the methods to improve the stability of HIPES is the addition of electrolytes to the aqueous phase. Aronson and Petko [13] studied the effect of electrolytes on properties and stability of HIPES. They found that the emulsion stability is improved by decreased solubility of aqueous phase in oil phase.

However, they concluded that even though Ostwald ripening contributed to HIPE destabilization and was prevented in the presence of the electrolyte, the coalescence is still dominant in HIPE instability. Kizling and Kronberg [14] suggested that lowering van der Waals interaction through polarizability or increasing the refractive index of the aqueous phase towards that of the oil phase could reduce the rate of coalescence.

HIPES have been investigated extensively for decades [15]–[19] and are used in a range of common practical applications in food, cosmetic formulations, drug delivery, and formation of porous materials [5], [7], [9]–[14], [20]. The most common application of HIPES is the synthesis of porous polymer as will be reviewed in next section.

1.4. Polymerization of High Internal Phase Emulsions

HIPES can be polymerized if one or both phases of the emulsion contain monomeric species [21]. This process yields a range of products with widely different properties. Emulsions can be used in three ways as a template for polymer synthesis: (i) polymerization of both phases (continuous and dispersed phases) to produce composites, (ii) polymerization of dispersed phase in order to produce colloidal particles, and (iii) polymerization of continuous phase and removing the dispersed phase to produce porous materials [22]. Polymerized High Internal Phase Emulsions also known as PolyHIPES, are usually produced by curing the continuous phase of HIPES. The continuous phase of emulsions should contain a cross-linker in addition to monomer and surfactant to provide the integrity to polyHIPE upon polymerization. The cross-linker forms the polymer network structure. Once cured, the dispersed phase is removed and the polyHIPE is washed by Soxhlet extractor and dried. If HIPE is stabilized by particles instead of surfactants, the product is known as poly-Pickering-HIPES [23]. Following polymerization of the continuous phase, the emulsion droplets are embedded in the resulting material. Under the correct conditions (*vide infra*), small interconnecting windows are formed between adjacent emulsion droplets upon

polymerization allowing the droplet phase to be removed by drying and form voids (where droplet were before) in the polyHIPE. Consequently, a highly porous and permeable material is produced with complex pore morphology [4]. Typical micrographs of HIPEs and polyHIPEs are shown in Figure 4.

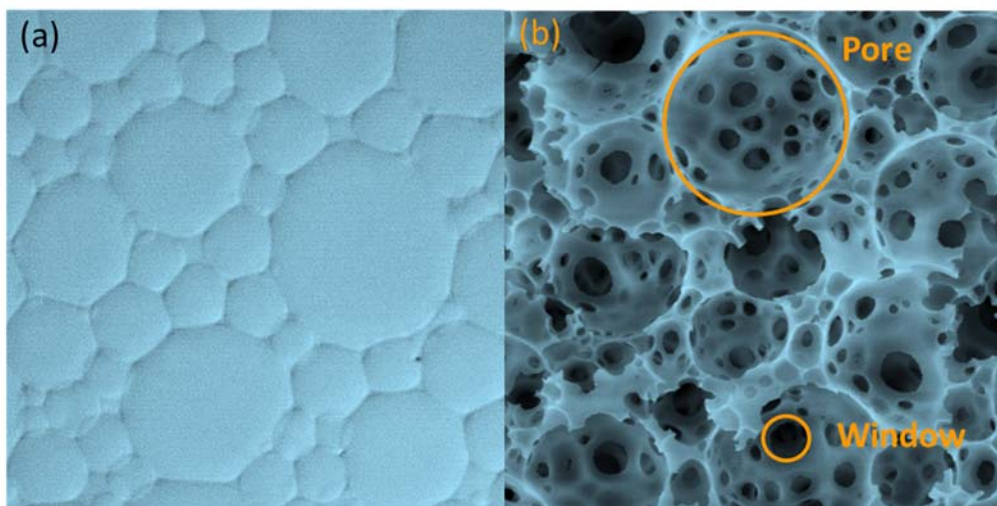


Figure 4. Typical micrographs of (a) HIPE and (b) polyHIPE [20]

The porous materials obtained from polymerization of HIPE are useful for a wide range of advanced applications, such as catalyst supports, ion-exchange modules, separation media, electrochemical sensing [5], supports for cell cultures, bone grafts, setting cement for oil well applications, porous electrodes [7], and separators in lithium ion batteries [8]. The open cellular morphology also makes the polyHIPE a potential candidate for thermal and acoustic insulation [5] within engine compartments and other enclosures. The highly interconnected macroporous structures can be advantageous for achieving high transport rates to microporous walls for molecular storage applications. They can also be formed into macroporous beads [10].

Because of flexibility of polyHIPEs to be produced in any shape and structure, controllable pore size, and high porosity (at least 74.05%), they have the potential to be utilized in liquid separation devices as membranes. Zhao et al. [24]

produced thin layers of polyHIPEs by reactive molding them between two flat plates, separated by poly(ethylene terephthalate) films. The other methods are the slicing the polyHIPE monoliths [25], and polymerization of blade-cast HIPEs on the support.

PolyHIPEs are mostly used as filter for protein purification or gas separation [24], [26]–[29]. Bhumgara [30] used HIPE to produce filter device with 48 cross-flow channels, by pumping a prepared HIPE into a mold before polymerization. The device could successfully filter calcium carbonate particles with 11 μm diameter. In addition, Krajnc et al. [28] produced monoliths for protein separation. The polyHIPE monoliths were modified to bear weak-anion exchange groups for separation of standard protein mixture containing myoglobin, conalbumine, and trypsin inhibitor. Good separation was achieved in a very short time similar to the separation obtained by commercial methacrylate monoliths. However, higher dispersion of protein was observed with polyHIPEs. The other separation application of polyHIPEs is as a permeable barrier with high mechanical properties in oil wells, replacing traditional gravel packs, which has been successfully produced by Ikem et al. [31].

Interaction between the mold and HIPE which results in a low permeability surface on final polyHIPE, as well as droplet coalescence during polymerization of HIPE are disadvantages of polymerizing thin layers of HIPE [27]. However, Krajnc et al. [32] could successfully produce a polyHIPE membrane with thickness between 30-500 μm . The oil phase of HIPEs contained styrene, divinylbenzene, vinylbenzyl chloride, and ethylhexyl acrylate. The pinhole-free membranes were prepared by casting HIPEs onto glass by using an appropriate blade. The mechanical flexibility of polyHIPEs was controlled by the degree of cross-linking and the addition of ethylhexyl acrylate.

2. Experimental

2.1. Materials

Butyl acrylate (BA, 99% , Sigma-Aldrich) and sodium acrylate (SA, 97%, Sigma- Aldrich) as monomers; sorbitane monooleate (Span 80, Sigma-Aldrich), Polyglycerol polyricinoleate (PGPR 4125, Palsgaard), and Pluronic L121 (BASF) as surfactants; divinylbenzene (DVB, 80%, Sigma-Aldrich) and ethylene glycol dimethacrylate (EGDMA, 98%, Sigma-Aldrich) as cross-linker; potassium persulfate (KPS, 99%, Acros) as thermal initiator; 1-hydroxycyclohexyl phenyl ketone (1-HPK, 99%, Sigma-Aldrich) as photo initiator; and benzoyl peroxide (BPO, 75%, Sigma-Aldrich) and N,N-dimethyl-p-toluidine (DMT, 99%, Sigma-Aldrich) as redox initiator were used as received. Structures of majorly used chemicals are shown in Figure 5.

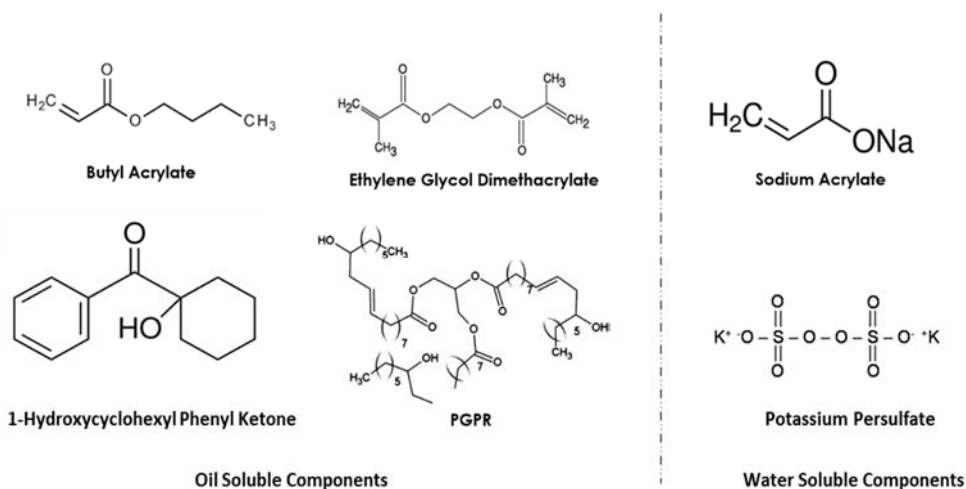


Figure 5. Structure of majorly used chemicals

2.2. Emulsion preparation

The oil phase of emulsion was a mixture of monomer (butyl acrylate), surfactant (PGPR 4125, Span80, or Pluronic L121) and cross-linker (EGDMA or DVB). For some samples photo-initiator (1-hydroxycyclohexyl phenyl ketones) or redox initiator (N,N-dimethyl-4-toluidine and benzoyl peroxide) were also added. Table 1 shows all samples in details. In this table volume fraction and composition of all samples are included.

Table 1. Composition of prepared samples and corresponding morphological observation

Sample Number	Oil Phase									Aqueous Phase				HIPE Formation	Open pore Formation	Window Formation
	Water Phase (wt. %)			Surfactant (wt.%)			Initiator (wt.%)			Monomer	Initiator (wt.%)		Salt			
	BA (ratio)	EDGMA (ratio)	DVB (ratio)	PGPR	Span 80	Pluronic L121	I-HPK	DMT (wt %)	SA (wt.%)		KPS	BPO				
1	75	3	1	-	10	-	-	-	-	-	0.5	-	2	Yes	Yes	Some
2	75	3	1	-	15	-	-	-	-	-	0.5	-	2	Yes	Yes	Some
3	75	3	1	-	20	-	-	-	-	-	0.5	-	2	Yes	Yes	Some
4	75	3	1	-	25	-	-	-	-	-	0.5	-	2	Yes	Yes	Some
5	75	3	1	-	30	-	-	-	-	-	0.5	-	2	Yes	Yes	Some
6	80	3	1	-	10	-	-	-	-	-	0.5	-	2	Yes	Yes	Some
7	80	3	1	-	15	-	-	-	-	-	0.5	-	2	Yes	Yes	Some
8	80	3	1	-	20	-	-	-	-	-	0.5	-	2	Yes	Yes	Some
9	80	3	1	-	25	-	-	-	-	-	0.5	-	2	Yes	Yes	Some
10	80	3	1	-	30	-	-	-	-	-	0.5	-	2	Yes	Yes	Some
11	85	3	1	-	10	-	-	-	-	-	0.5	-	2	Yes	Yes	Some
12	85	3	1	-	15	-	-	-	-	-	0.5	-	2	Yes	Yes	Some
13	85	3	1	-	20	-	-	-	-	-	0.5	-	2	Yes	Yes	Some
14	85	3	1	-	25	-	-	-	-	-	0.5	-	2	Yes	Yes	Some
15	85	3	1	-	30	-	-	-	-	-	0.5	-	2	Yes	Yes	Some
16	85	3	1	-	10	-	-	-	-	-	0.5	-	2	Yes	Yes	Some
17	90	3	1	-	10	-	-	-	-	-	0.5	-	2	Yes	Yes	Some
18	90	3	1	-	15	-	-	-	-	-	0.5	-	2	Yes	Yes	Some
19	90	3	1	-	20	-	-	-	-	-	0.5	-	2	Yes	Yes	Some
20	90	3	1	-	25	-	-	-	-	-	0.5	-	2	Yes	Yes	Some
21	90	3	1	-	30	-	-	-	-	-	0.5	-	2	Yes	Yes	Some
22	90	3	1	-	10	-	-	-	-	-	0.5	-	2	No	-	-
23	95	3	1	-	10	-	-	-	-	-	0.5	-	2	No	-	-
24	95	3	1	-	15	-	-	-	-	-	0.5	-	2	No	-	-
25	95	3	1	-	20	-	-	-	-	-	0.5	-	2	No	-	-
26	95	3	1	-	25	-	-	-	-	-	0.5	-	2	No	-	-
27	95	3	1	-	30	-	-	-	-	-	0.5	-	2	No	-	-
28	90	3	1	-	10	-	-	-	-	-	0.5	-	5	No	-	-
29	90	3	1	-	15	-	-	-	-	-	0.5	-	5	No	-	-
30	90	3	1	-	20	-	-	-	-	-	0.5	-	5	No	-	-

Sample Number	Water Phase (wt. %)	Oil Phase								Aqueous Phase				HIPE Formation	Open pore Formation	Window Formation	
		Monomer		Cross-linker		Surfactant (wt.%)			Initiator (wt.%)		Monomer	Initiator (wt.%)					Salt
		BA (ratio)	EDGMA (ratio)	DVB (ratio)	PGPR	Span 80	Pluronic L121	1-HPK	DMT (wt %)	SA (wt.%)	KPS	BPO	NaCl (wt.%)				
31	90	3	1	-	25	-	-	-	-	-	0.5	-	5	No	-	-	
32	90	3	1	-	30	-	-	-	-	-	0.5	-	5	No	-	-	
33	90	3	1	-	10	-	-	-	-	-	0.5	-	5	No	-	-	
34	95	3	1	-	10	-	-	-	-	-	0.5	-	5	No	-	-	
35	95	3	1	-	15	-	-	-	-	-	0.5	-	5	No	-	-	
36	95	3	1	-	20	-	-	-	-	-	0.5	-	5	No	-	-	
37	95	3	1	-	25	-	-	-	-	-	0.5	-	5	No	-	-	
38	95	3	1	-	30	-	-	-	-	-	0.5	-	5	No	-	-	
39	75	3	1	-	30	-	-	-	-	0.5	0.5	-	2	Yes	Yes	Some	
40	80	3	1	-	30	-	-	-	-	0.5	0.5	-	2	Yes	Yes	Some	
41	85	3	1	-	30	-	-	-	-	0.5	0.5	-	2	Yes	Yes	Some	
42	90	3	1	-	30	-	-	-	-	0.5	0.5	-	2	Yes	Yes	Some	
43	95	3	1	-	30	-	-	-	-	0.5	0.5	-	2	Yes	Yes	Some	
44	75	3	1	-	30	-	-	-	-	1	0.5	-	2	Yes	Yes	Some	
45	80	3	1	-	30	-	-	-	-	1	0.5	-	2	Yes	Yes	Some	
46	85	3	1	-	30	-	-	-	-	1	0.5	-	2	Yes	Yes	Some	
47	90	3	1	-	30	-	-	-	-	1	0.5	-	2	Yes	Yes	Some	
48	95	3	1	-	30	-	-	-	-	1	0.5	-	2	Yes	Yes	Some	
49	75	3	1	-	30	-	-	-	-	2	0.5	-	2	Yes	Yes	Some	
50	80	3	1	-	30	-	-	-	-	2	0.5	-	2	Yes	Yes	Some	
51	85	3	1	-	30	-	-	-	-	2	0.5	-	2	Yes	Yes	Some	
52	90	3	1	-	30	-	-	-	-	2	0.5	-	2	Yes	Yes	Some	
53	95	3	1	-	30	-	-	-	-	2	0.5	-	2	Yes	Yes	Some	
54	75	3	-	1	-	10	-	-	-	-	0.5	-	5	No	-	-	
55	75	3	-	1	-	15	-	-	-	-	0.5	-	5	No	-	-	
56	75	3	-	1	-	20	-	-	-	-	0.5	-	5	No	-	-	
57	75	3	-	1	-	25	-	-	-	-	0.5	-	5	No	-	-	
58	75	3	-	1	-	30	-	-	-	-	0.5	-	5	some	-	-	
59	75	3	-	1	-	35	-	-	-	-	0.5	-	5	Yes	Yes	Yes	
60	80	3	-	1	-	35	-	-	-	-	0.5	-	5	Yes	Yes	Yes	
61	85	3	-	1	-	35	-	-	-	-	0.5	-	5	Yes	Yes	Yes	

Sample Number	Water Phase (wt. %)	Oil Phase								Aqueous Phase				HIPE Formation	Open pore Formation	Window Formation		
		Monomer		Cross-linker		Surfactant (wt.%)			Initiator (wt.%)		Monomer		Initiator (wt.%)				Salt	
		BA (ratio)	EDGMA (ratio)	DVB (ratio)	PGPR	Span 80	Pluronic L121	1-HPK	DMT (wt %)	SA (wt.%)	KPS	BPO	NaCl (wt.%)					
62	90	3	-	1	-	35	-	-	-	-	0.5	-	5	Yes	Yes	Yes		
63	95	3	-	1	-	35	-	-	-	-	0.5	-	5	No	-	-		
64	75	3	1	-	-	-	10	-	-	-	0.5	-	5	No	-	-		
65	75	3	1	-	-	-	15	-	-	-	0.5	-	5	No	-	-		
66	75	3	1	-	-	-	20	-	-	-	0.5	-	5	No	-	-		
67	75	3	1	-	-	-	25	-	-	-	0.5	-	5	No	-	-		
68	75	3	1	-	-	-	30	-	-	-	0.5	-	5	some	-	-		
69	75	3	1	-	-	-	35	-	-	-	0.5	-	5	Yes	Yes	Some		
70	80	3	1	-	-	-	35	-	-	-	0.5	-	5	Yes	Yes	Some		
71	85	3	1	-	-	-	35	-	-	-	0.5	-	5	Yes	Yes	Some		
72	90	3	1	-	-	-	35	-	-	-	0.5	-	5	No	-	-		
73	95	3	1	-	-	-	35	-	-	-	0.5	-	5	No	-	-		
74	75	3	1	-	20	-	-	0.5	-	-	-	-	5	No	-	-		
75	80	3	1	-	20	-	-	0.5	-	-	-	-	5	No	-	-		
76	85	3	1	-	20	-	-	0.5	-	-	-	-	5	No	-	-		
77	90	3	1	-	20	-	-	0.5	-	-	-	-	5	No	-	-		
78	95	3	1	-	20	-	-	0.5	-	-	-	-	5	No	-	-		
79	75	3	1	-	20	-	-	-	0.25	-	-	0.25	5	No	-	-		
80	80	3	1	-	20	-	-	-	0.25	-	-	0.25	5	No	-	-		
81	85	3	1	-	20	-	-	-	0.25	-	-	0.25	5	No	-	-		
82	90	3	1	-	20	-	-	-	0.25	-	-	0.25	5	No	-	-		
83	95	3	1	-	20	-	-	-	0.25	-	-	0.25	5	No	-	-		
84	75	3	1	-	30	-	-	0.25	-	-	0.25	-	5	Yes	Yes	Yes		
85	80	3	1	-	30	-	-	0.25	-	-	0.25	-	5	Yes	Yes	Yes		
86	85	3	1	-	30	-	-	0.25	-	-	0.25	-	5	Yes	Yes	Yes		
87	90	3	1	-	30	-	-	0.25	-	-	0.25	-	5	No	-	-		
88	95	3	1	-	30	-	-	0.25	-	-	0.25	-	5	No	-	-		
89	75	3	1	-	30	-	-	0.25	-	0.5	0.25	-	5	Yes	Yes	Yes		
90	80	3	1	-	30	-	-	0.25	-	0.5	0.25	-	5	Yes	Yes	Yes		
91	85	3	1	-	30	-	-	0.25	-	0.5	0.25	-	5	Yes	Yes	Yes		
92	75	3	1	-	30	-	-	0.25	-	1	0.25	-	5	Yes	Yes	Yes		

Sample Number	Water Phase (wt. %)	Oil Phase								Aqueous Phase				HIPE Formation	Open pore Formation	Window Formation		
		Monomer		Cross-linker		Surfactant (wt.%)			Initiator (wt.%)		Monomer		Initiator (wt.%)				Salt	
		BA (ratio)	EDGMA (ratio)	DVB (ratio)	PGPR	Span 80	Pluronic L121	1-HPK	DMT (wt %)	SA (wt.%)	KPS	BPO	NaCl (wt.%)					
93	80	3	1	-	30	-	-	0.25	-	1	0.25	-	5	Yes	Yes	Yes		
94	85	3	1	-	30	-	-	0.25	-	1	0.25	-	5	Yes	Yes	Yes		
95	75	3	1	-	30	-	-	0.25	-	2	0.25	-	5	Yes	Yes	Yes		
96	80	3	1	-	30	-	-	0.25	-	2	0.25	-	5	Yes	Yes	Yes		
97	85	3	1	-	30	-	-	0.25	-	2	0.25	-	5	Yes	Yes	Yes		
98	75	3	1	-	35	-	-	0.25	-	-	0.25	-	5	Yes	Yes	Yes		
99	80	3	1	-	35	-	-	0.25	-	-	0.25	-	5	Yes	Yes	Yes		
100	85	3	1	-	35	-	-	0.25	-	-	0.25	-	5	Yes	Yes	Yes		
101	75	3	1	-	35	-	-	0.25	-	0.5	0.25	-	5	Yes	Yes	Yes		
102	80	3	1	-	35	-	-	0.25	-	0.5	0.25	-	5	Yes	Yes	Yes		
103	85	3	1	-	35	-	-	0.25	-	0.5	0.25	-	5	Yes	Yes	Yes		
104	75	3	1	-	35	-	-	0.25	-	1	0.25	-	5	Yes	Yes	Yes		
105	80	3	1	-	35	-	-	0.25	-	1	0.25	-	5	Yes	Yes	Yes		
106	85	3	1	-	35	-	-	0.25	-	1	0.25	-	5	Yes	Yes	Yes		
107	75	3	1	-	35	-	-	0.25	-	2	0.25	-	5	Yes	Yes	Yes		
108	80	3	1	-	35	-	-	0.25	-	2	0.25	-	5	Yes	Yes	Yes		
109	85	3	1	-	35	-	-	0.25	-	2	0.25	-	5	Yes	Yes	Yes		

The oil phase with different weight fractions was mixed with overhead mixer with 500 rpm for 10 minutes. Then, aqueous phase containing water, salt (NaCl) as stabilizer, and thermal initiators (KPS) if present was added dropwise to the oil phase. In some samples, second monomer (sodium acrylate) was also included in the aqueous phase. The weight fraction of aqueous phase was varied from 75 to 95%. Three last columns of Table 1 summarize the result of experiments, which will be elaborated in the Results and Discussion section. Some compositions could not form high internal phase emulsion and after a while one of instability processes (as schematically shown in Figure 2), mostly phase inversion, took place. In other words, HIPE formation is a critical step before one can synthesize

polyHIPE. Since window formation and open-pore structure have direct effect on permeability of membrane, they are also addressed in Table 1.

2.3. Sample preparation

After preparation of HIPEs, they should be polymerized to produce porous materials. In the case of thermal initiators, the samples were placed in an oven (Thermo Scientific, Heratherm oven, as shown in Figure 6) at temperature of 65-70 °C for 2 h. For photo-initiation, the samples were placed in a UV chamber (Spectroline, Select Series, as shown in Figure 7) at wavelength of 240 nm for 2 h.



Figure 6. Oven used to polymerize samples containing thermal initiator

For redox initiation, two different emulsions were prepared, each of them containing one component of redox initiator (either BPO or DMT). Then, these two emulsions were mixed together and placed under foam hood for 24 h for polymerization to be completed. The process of polyHIPE synthesis is schematically shown in Figure 8 and the setup used for HIPE preparation is shown in Figure 9.



Figure 7. UV cross-linker used to polymerize samples containing photo initiator

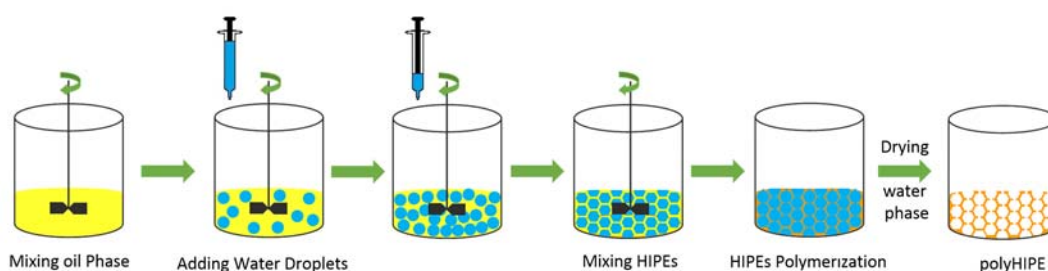


Figure 8. Schematic process of polyHIPE synthesis.

For thin-layer polyHIPE which is needed for membrane performance test, HIPE samples were cast on the support which was recovered from a commercial membrane (GE, MW series, MW2540F30) through washing with chloroform in Soxhlet for 24 h. The HIPE samples were cast on the support by sandwiching the support, HIPE, and a frame with 0.2 mm thickness between two stainless steel plates covered with Mylar sheets. Then, a constant pressure of 0.4 MPa was applied by a mechanical press to prepare a uniform thickness of HIPE and improve its diffusion in the support. Figure 10 shows the casting process schematically. Afterwards, samples were cured by UV and/or heating as will be discussed in the Results and Discussion.

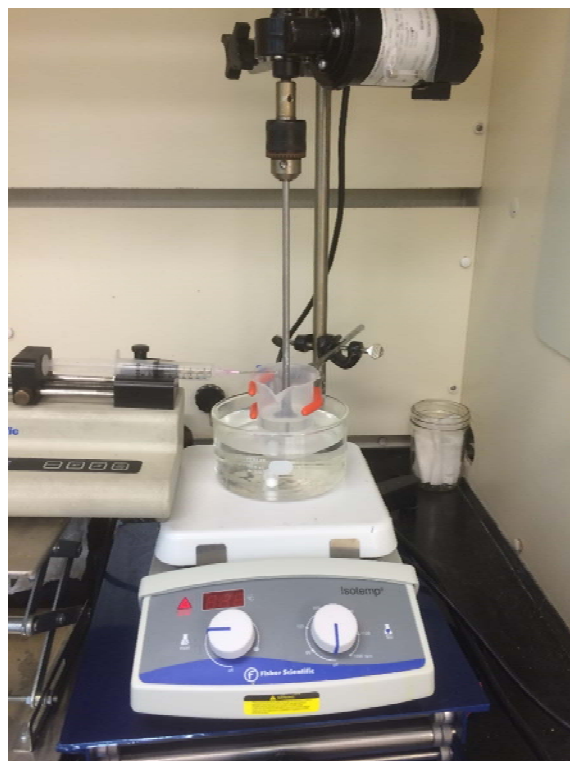


Figure 9. HIPE preparation setup

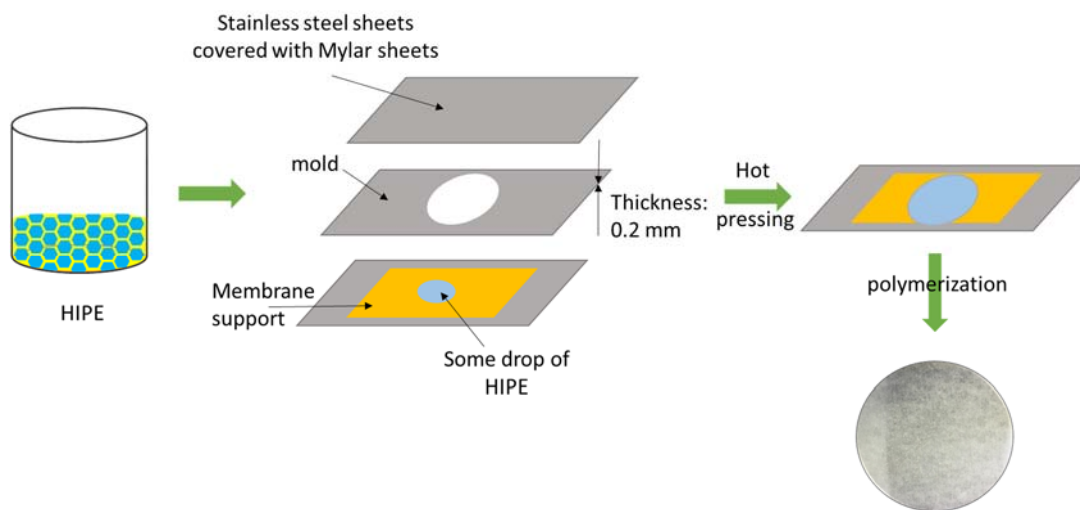


Figure 10. Casting thin layer of HIPE on support for membrane applications

All samples after polymerization were washed first with DI water for 24 h, and then with 2-propanol for another 24 h by a Soxhlet apparatus (shown in Figure 11).

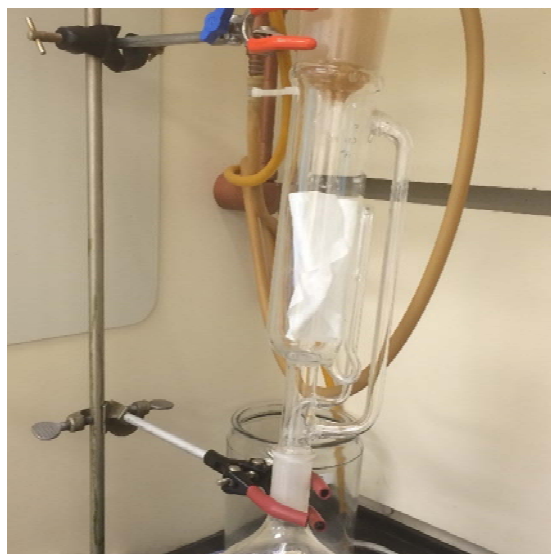


Figure 11. Soxhlet setup for washing polyHIPEs

2.4. Characterization

2.4.1. Morphology

As a primary characterization, morphology of prepared samples was studied to define a proper formulation of polyHIPE with desired structure (based on pore sizes and window formation). Scanning electron microscopy (SEM, S-3400N Type II, Hitachi High-Technologies Corp.) and optical microscopy (Nikon, Eclipse E400) were used to observe the morphology of polyHIPE and HIPE samples, respectively. The samples for optical microscopy were prepared by putting a drop of HIPE between a glass slide and a cover glass.

Sample preparation for SEM was performed by fracturing the dried polyHIPE in liquid nitrogen. Then, a piece of fractured sample was adhered on the sample holder with carbon conductive tape, and coated through gold sputtering.

2.4.2. Surface Chemistry

Fourier transform infrared spectroscopy (FTIR, Perkin-Elmer Spectrum One FTIR Spectrometer), and surface charge were investigated for characterizing the surface properties of polyHIPEs.

Surface charge density of membranes was studied by conductometric titration. PolyHIPE samples were grinded and dispersed in water (10 wt.%) 30 min before starting the experiment. The pH and conductivity of dispersion was recorded simultaneously by ultra pH/conductivity meter (hq40d, Hach Co.). A magnetic stirrer was used to continuously mix the dispersion. The HCL 0.1 N and NaOH 0.1 N were used for titration. The setup is shown in Figure 12.



Figure 12. conductometric titration setup

2.4.3. Mechanical Properties

Mechanical properties of selected samples were studied by compression test with mechanical tester machine (AGS-X, Shimadzu Co., shown in Figure 13) to determine the tolerance of samples to filtration pressures. PolyHIPE monoliths were cut into cylinders with 2.5 cm height and 1.5 cm diameter. Then, they placed between two plates of mechanical tester machine and compressing test was started with speed of 1 mm/min.



Figure 13. Mechanical tester equipment used to determine the resistance of membranes against pressure

2.4.4. Filtration test

A home-made setup was used for filtration measurement (Figure 14). Two sets of experiments were performed. First, the water flux was measured to calculate the permeability of prepared membranes. In the second experiment, the capabilities of polyHIPE membrane to remove suspended oil droplets was studied by filtering a mixture of vegetable oil (25g), NaCl (500 mg), Pluronic F68 (5 g) and DI water (1L). This mixture was prepared through stirring prior to filtration by a magnetic stirrer bar (3/8 in. diameter, 2 in. length) in a 1 L flat-bottom Erlenmeyer flask at a constant speed of 600 rpm at 60°C for 24 h [12]. Additionally, for particle filtration, another feed mixture containing 10 wt.% talc, $\text{H}_2\text{Mg}_3(\text{SiO}_3)_4$, was prepared. Since talc is insoluble in water, 2 wt.% Pluronic F 68 was also added to stabilize the suspension.

The permeability of polyHIPEs can also be measured through drying kinetics test after saturation with water. PolyHIPEs after washing with 2-propanol and water were dried in the oven at 45°C for 48 h and then immersed in DI water for 6h. Each sample was weighted after saturation with water, and then placed in the

oven. The drying kinetics of samples was obtained by measuring their weight in 30 min intervals.



Figure 14. Homemade filtration setup

3. Results and Discussion

3.1. Morphology

PolyHIPEs as membrane have potential application for filtration of suspending particles and bacteria. To produce optimum morphology, several formulations were synthesized as summarized in Table 1. Since the pore size and pore formation are controlled by droplet size of emulsion in HIPE templating, the time of mixing, speed of mixing, and surfactant concentration (10-35 wt%) were varied from 0-90 min, 400-650 rpm, and 10-35 wt.% in different formulations, respectively. For example, as shown in Figure 15, by increasing the mixing time, the droplet size is decreased.

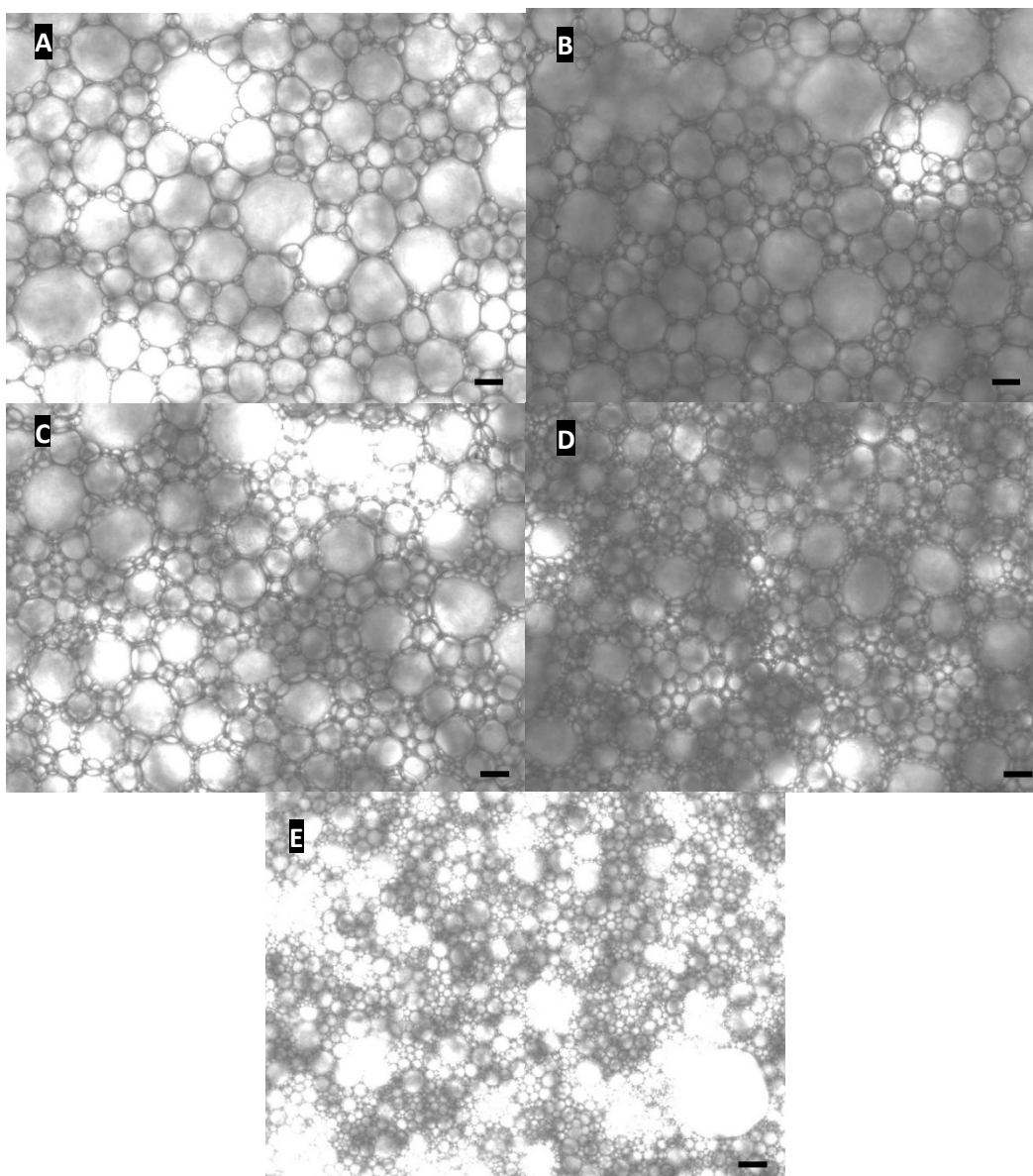


Figure 15. Optical micrographs of sample #17 after A) 0 min, B) 5 min, C) 10 min, D) 30 min, and E) 60 min of mixing. The scale bar is equal to 10 μm .

The concentration and type of surfactant affect the stability of emulsion. For example as shown in Table 1, the water does not emulsify in oil containing Span 80 as a surfactant with concentration lower than 30%. The stability of emulsions were investigated through monitoring their morphology with time. The variation of surfactant concentration shows two satisfactory observations: (i) higher

stability of emulsions (as shown in Figure 16), and (ii) smaller droplet sizes (discussed below) by increasing the surfactant concentration.

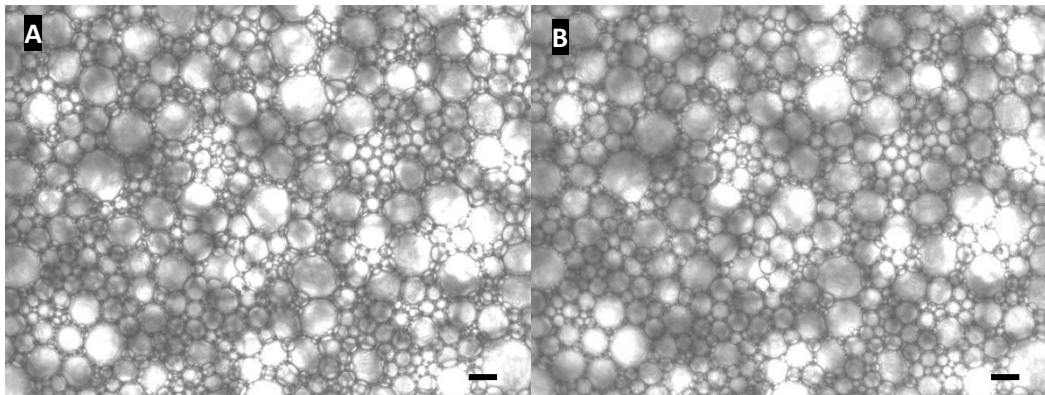


Figure 16. Optical microscopy of sample #27: A) 0 min, and B) 5 min after casting on glass slide. The scale bar is equal to 10 μm .

The second method to study the stability of HIPE is to compare the droplet sizes of HIPE (by optical microscopy before polymerization) and the void size of polyHIPE (by SEM after polymerization) since polymerization with thermal initiation may affect the stability of emulsions and final microstructure in polyHIPE. As seen in Figure 16, the domain size of sample 14 increases upon polymerization (note that the scale bar in SEM micrograph is equal to 50 μm , while it is equal to 10 μm in optical micrograph), which can be attributed to the increase in coalescence rate at high temperatures. To overcome this shortcoming, a photo-initiator was incorporated in formulations (sample 74-78). The role of photo-polymerization is to set the HIPE structure in the absence of intensive thermal initiation. We observed that HIPE samples cannot be prepared only via photo-polymerization (see for instant #74 to 78 in Table 1) since the white color of emulsions limits the penetration length of UV light. Therefore, a combination of thermal and photo-polymerization was investigated (sample 79-97 in Table 1). In other words, photo-polymerization as pre-polymerization stage was firstly performed and then thermal polymerization was used to complete the curing of samples. Additionally, we observed that increasing the salt concentration from 2

wt.% to 5 wt.% in the water phase improves the stability of HIPE during polymerization (by comparing sample #1 and #54).

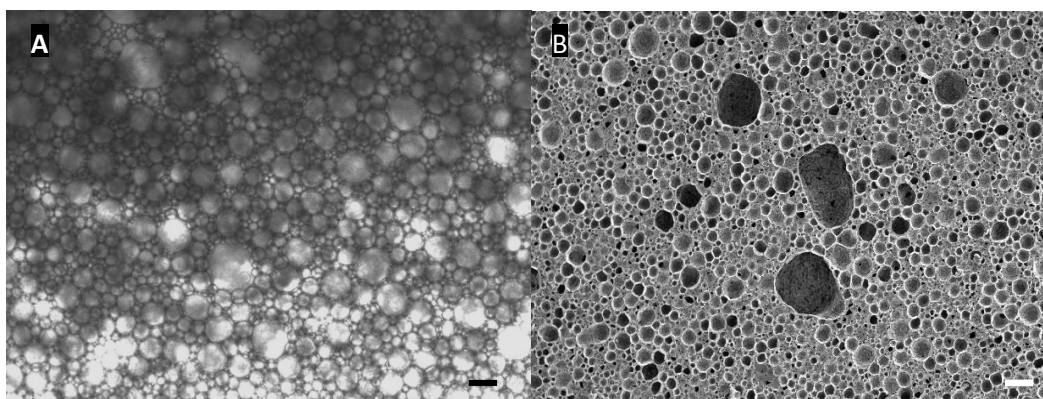


Figure 17. Comparison of (A) droplet size of HIPE before polymerization obtained by optical microscopy (scale bar: 10 μm), and (B) void size of polyHIPE after polymerization obtained by SEM (scale bar: 50 μm) for sample #14.

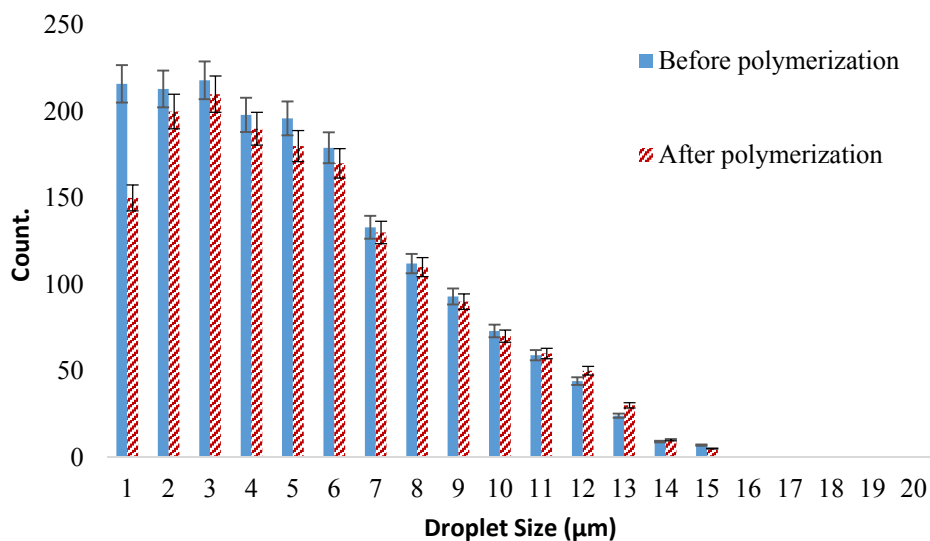


Figure 18. Droplet/void size distribution before and after polymerization (Sample #100)

To quantify the stability of emulsions, droplet size distributions before and after polymerization were investigated through image analysis of optical micrographs and scanning electron micrographs, respectively. As seen in Figure 17, the size distribution does not change in the sample that goes through first

photo- and then thermal polymerization. Therefore, the developed method of combined initiation in this work can successfully be employed in the scale-up of process.

Since window size directly affects the permeability of polyHIPE membranes, different formulations were made to produce different windows as shown in Figure 18.

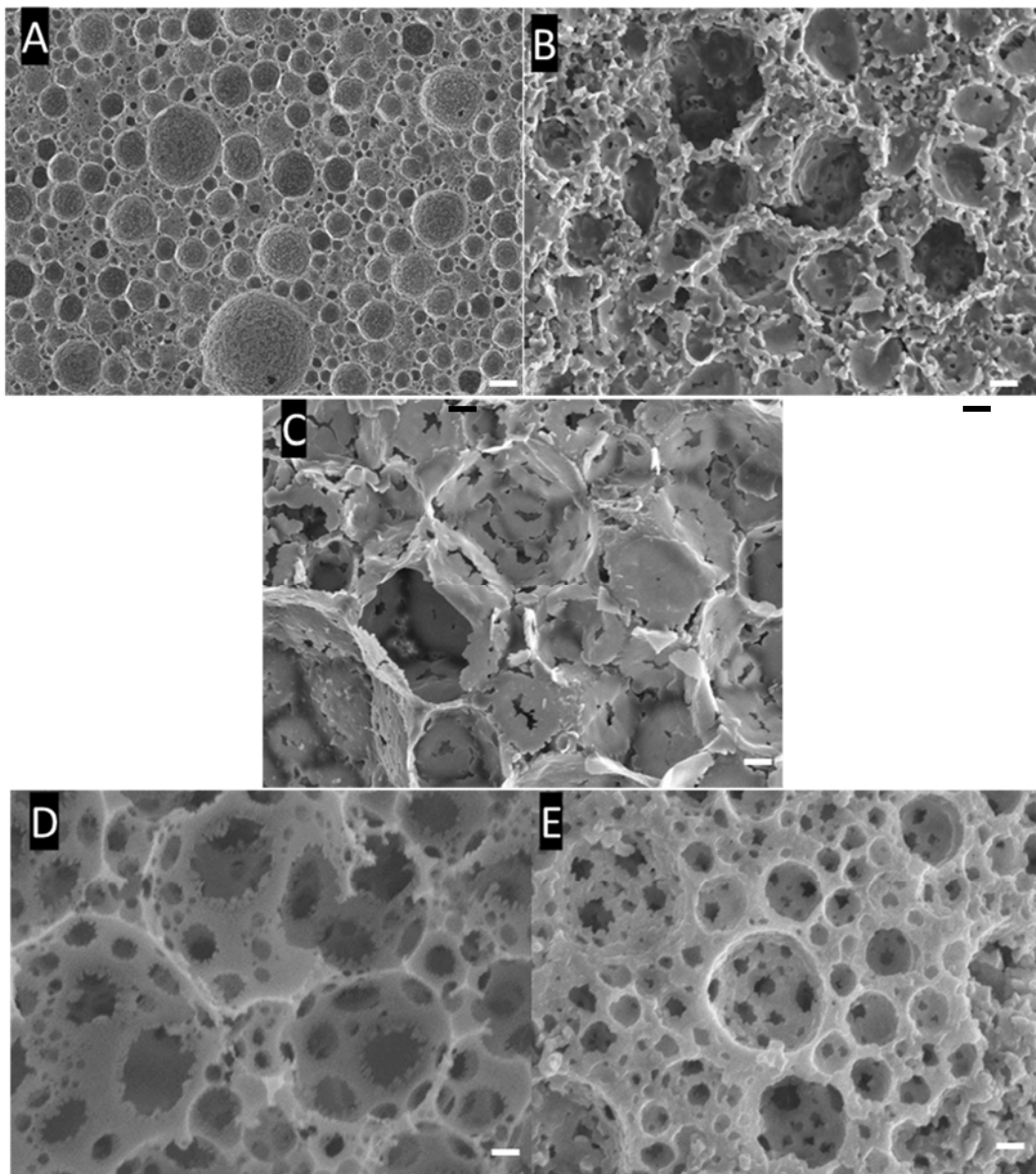


Figure 19. Different window formation: A) SEM of sample #26: no window formation, B) SEM of sample #35: some window formation, C) SEM of sample #46: some window formation, D) SEM of sample #62: large window formation, E) SEM of sample #100: intermediate window formation in term of size and volume. The scale bar is equal to $5\mu\text{m}$.

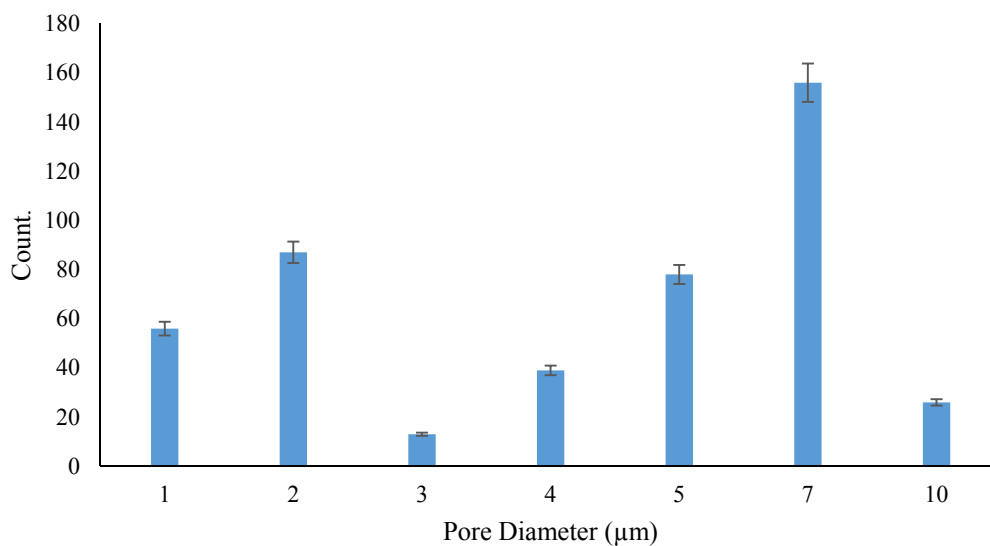


Figure 20. Pore size distribution of sample #100

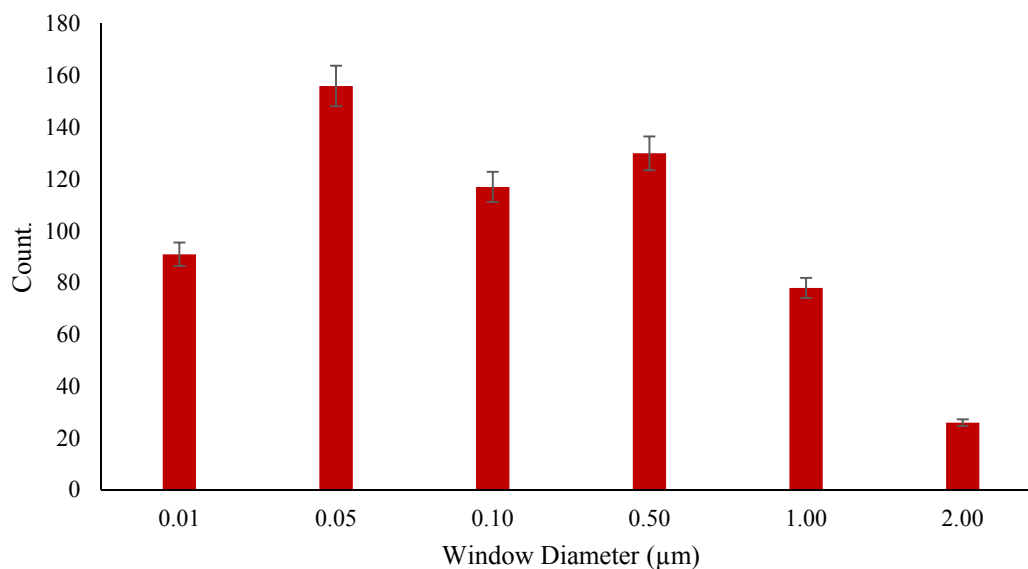


Figure 21. Window size distribution of sample #100

The size distribution of pores and windows was investigated for sample #100 – which was found to be the optimum formulation in terms of stability, polymerization, and window formation – as shown in Figure 20 and 21. This sample has window size between 0.01 to 1 μm. Therefore, membranes made from

this polyHIPE are on the upper bond of ultrafiltration and can be also utilized as microfiltration membranes.

3.2. In-situ functionalization

For water purification, the ideal ultrafiltration and microfiltration membranes should have hydrophilic surface and hydrophobic structure, because: (i) the hydrophilic surface will interact with water and reject the hydrophobic particles which in turn decrease the fouling, and (ii) a hydrophilic body of membrane will result in swelling of membrane during filtration which will decrease its performance. Therefore, surface of commercialized membranes is usually treated. In this study, for the first time the surface modification is performed in-situ, which means during the polymerization of membrane.

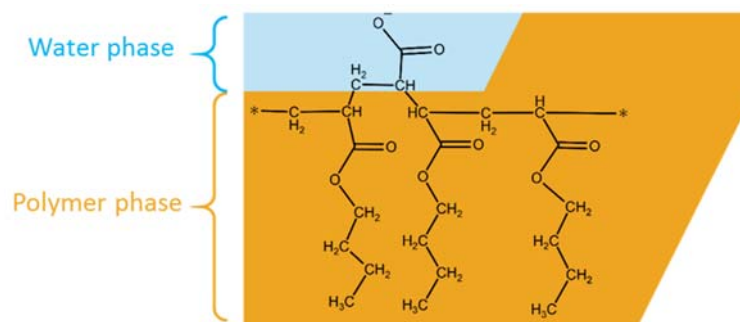


Figure 22. Schematic of in-situ functionalization process of polyHIPE developed in this work

The nature of synthesized polyHIPE membrane is hydrophobic (the employed monomers form hydrophobic polymer); therefore, a water-soluble monomer (sodium acrylate) was added in the aqueous phase to produce a hydrophilic surface during polymerization as schematically shown in Figure 22. In addition, the employed surfactant has unsaturated carbon-carbon bonds, and thus, can be copolymerized with continuous phase.

The FTIR of two samples (#21 and #47) are shown in Figure 23 and 24. Sodium acrylate has O^- functional group while butyl acrylate does not; therefore,

the observed broad peak in $3200-3600\text{ cm}^{-1}$ in FTIR of samples can be due to the $-\text{O}-$ group belongs to sodium acrylate at the surface and/or the $-\text{OH}$ functional group of PGPR surfactant.

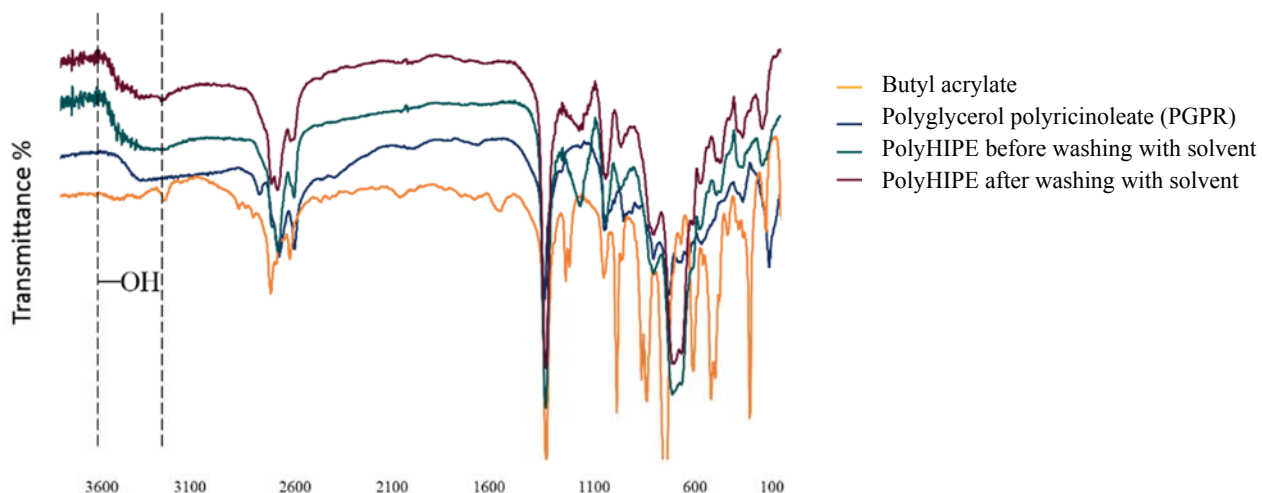


Figure 23. Comparing FTIR results of polyHIPE before and after washing with solvent to study the reactivity of surfactant (sample #21)

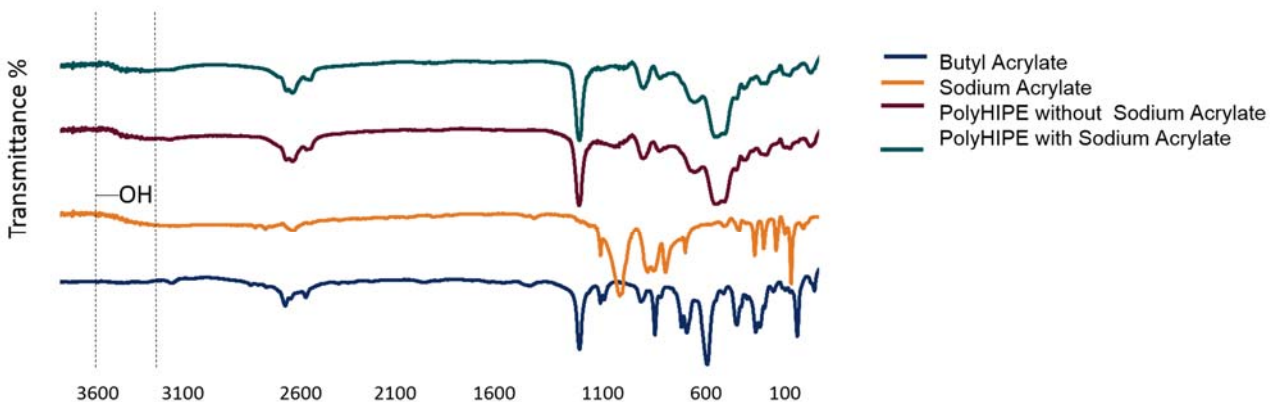


Figure 24. FTIR results show change in surface chemistry for polyHIPEs with (sample #47) and without sodium acrylate (sample #21)

FTIR results in Figure 23 shows that even after washing samples with 2-propanol which dissolves PGPR, the peaks in the $3200\text{ to }3600\text{ cm}^{-1}$ range are still present in polyHIPE sample. PGPR also shows similar peaks in the same range.

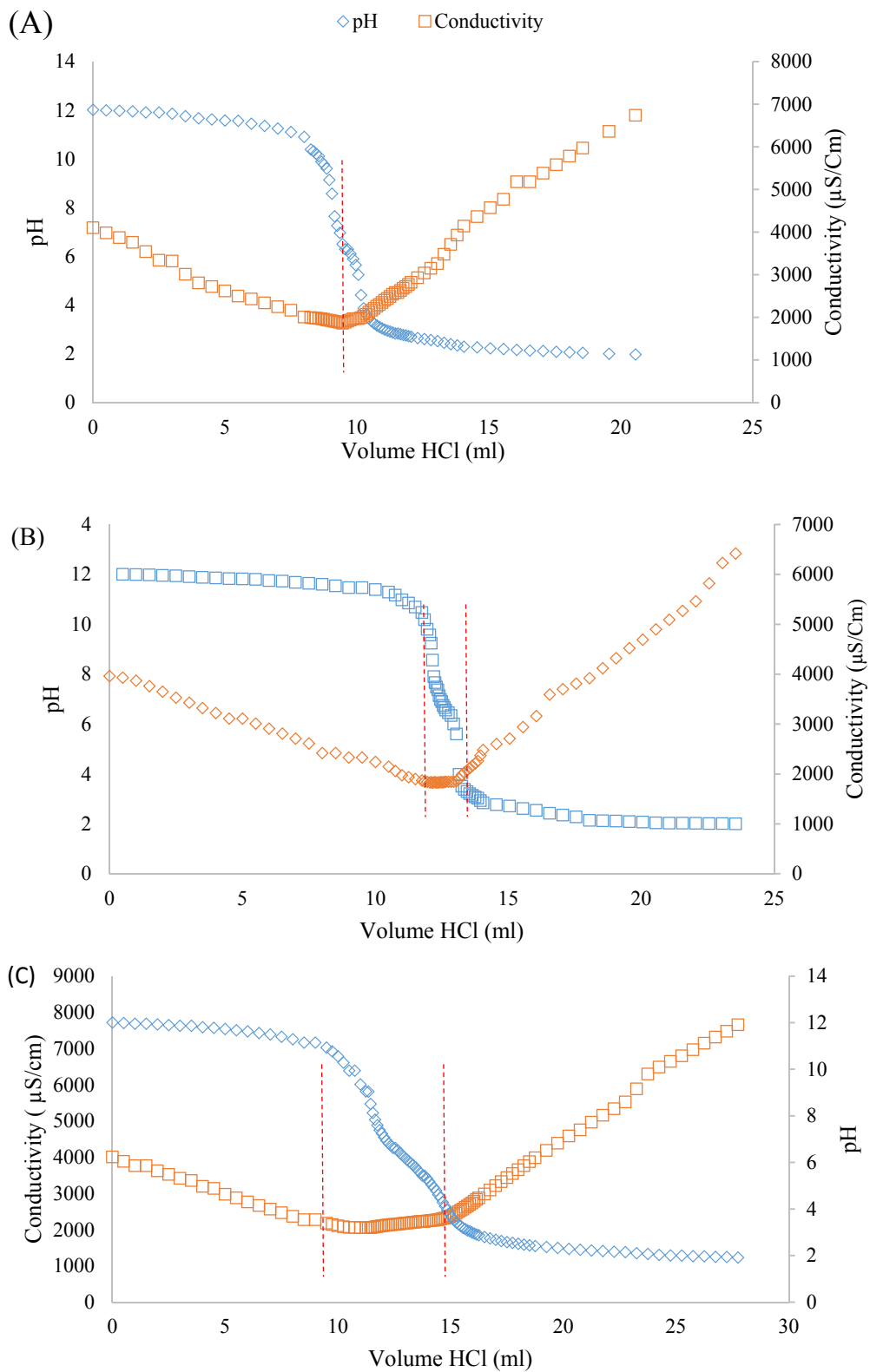


Figure 25. Titration curve for: (A) DI water, (B) polyHIPE without sodium acrylate, and (C) polyHIPE with 1 wt.% sodium acrylate

The results in Figure 23 confirm that the surfactant is copolymerized with BA and EGDMA through the existing double bonds in its chemical structure. In Figure 24, the FTIR results of polyHIPE with/without SA are presented. The peak in the 3200 to 3600 cm^{-1} range as seen in Figure 23 appears in both samples, which shows that SA may also reacted with BA. To confirm the copolymerization of SA with continuous phase at the surface of polyHIPE, the charge density of polyHIPE is also studied by conductometric titration (Figure 25).

Comparing the charge density of membranes without and with sodium acrylate in the formulation, as shown in Table 2, shows that the charge density increases by increasing the percentage of sodium acrylate in the continuous phase. The results confirm that by adding sodium acrylate to the aqueous phase, in-situ functionalization takes place. The titration results also show that the polyHIPE without sodium acrylate (sample #100) has some surface charge which can be related to the copolymerization of PGPR with continuous phase. It should be noted that DI water was tested as control sample to make sure that the obtained results are not artifact.

Table 2. Charge density for samples No. 103, 106, 109

Sample	Charge Density (C.m^{-2})
Control (DI water)	0
PolyHIPE without SA (sample #100)	0.45
PolyHIPE with 1% SA (sample #106)	1.92
PolyHIPE with 2% SA (sample #109)	3.16

3.3. Mechanical properties

One of the important properties of ultrafiltration and microfiltration membranes is mechanical properties since the filtration process is normally done

at high pressures (around 5 to 10 bar, equal to 0.5 to 1 MPa). As shown in Figure 25, by increasing the volume fraction, mechanical properties is decreased. However, even the sample with the lowest mechanical properties in this study is strong enough to withstand the pressure of filtration process.

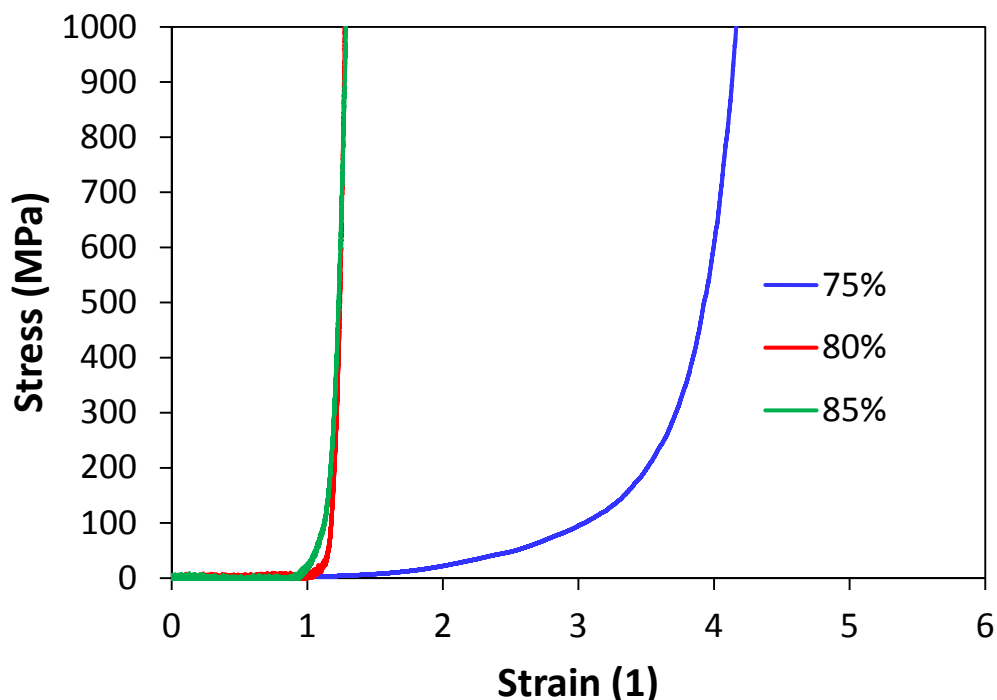


Figure 26. Stress versus strain curve of polyHIPE with different pore volume fraction (samples #89, 90, and 91)

3.4. Permeability

Performance of synthesized membranes was evaluated by carrying out pure water permeation, flux and rejection, and drying kinetics. Pure water permeation and drying kinetics are directly related to the membrane pore size and porosity, and thus its permeability. However, the permeate flux is influenced by several other factors such as feed solute molecular weight, feed concentration, and solute physical structure. Pure water permeation was studied based on Darcy's coefficient by dead-end filtration setup. Darcy's law was used to calculate the permeability as follows:

$$\frac{\kappa}{l} = \frac{Q \mu}{A \Delta P}$$

where, Q , μ , A , ΔP , l , and κ are flow rate, viscosity, membrane area, pressure difference along the membrane, membrane thickness, and Darcy's constant (which features intrinsic permeability), respectively. The ratio of κ/l was considered as an indication of operational permeability in this work. In other words, since different membranes may have different thicknesses which is also difficult to be accurately measured, the value of intrinsic permeability itself can be misleading in real application.

The results are shown in Table 3, in which the synthesized membranes show higher permeability than commercial UF membranes due to high porosity of polyHIPEs. Therefore, UF/MF membranes can successfully be produced from HIPE templating not only with potential to utilize different monomers but also with higher permeability. In addition, the fabrication of polyHIPE membranes is ecofriendly since it uses water to generate pores instead of organic solvent.

The kinetics of drying was also studied, which shows that by adding SA, because of hydrophilic surface, the drying process is faster (higher slope at short times) as shown in Figure 27.

Table 3. Pure water permeation result based on Darcy's law

	Sample #100	Sample #103	Sample #106	Sample #109	Commercial UF (GE)
P atm (KPa)	101	101	101	101	101
P pump (KPa)	482	965	517	482	1200
Area (mm ²)	1380	1380	1380	1380	1380
Q (ml/sec)	26.316	31.250	29.412	30.303	1.0
Thickness (mm)	0.2	0.2	0.2	0.2	0.2
κ/l (m)	5.02×10^{-11}	2.63×10^{-11}	5.13×10^{-11}	5.77×10^{-11}	6.61×10^{-13}

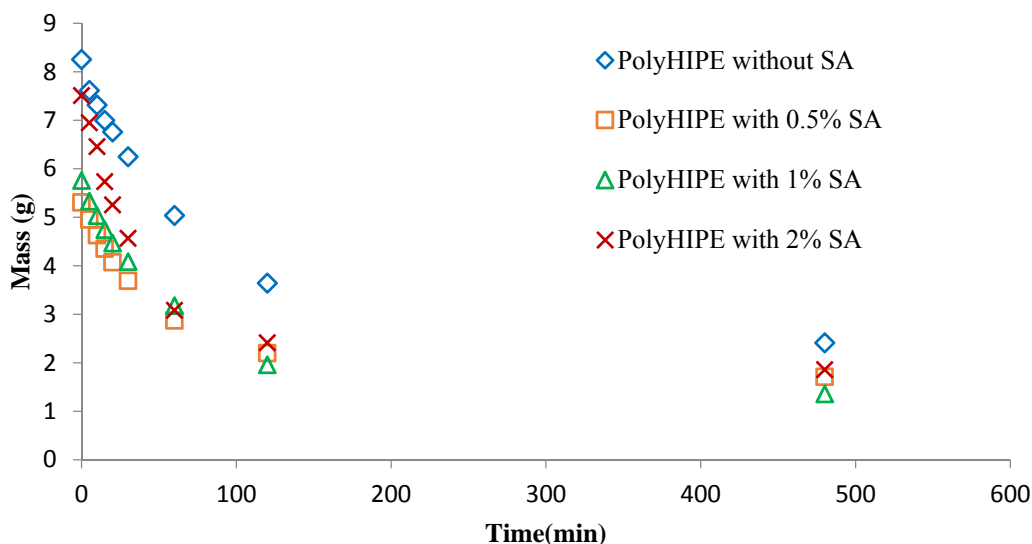


Figure 27. Drying kinetics of polyHIPE without (sample #10), with 0.5% (sample #40), with 1% (sample #45), and with 2% (sample #50) sodium acrylate

After studying the water flux permeation, permeability for filtering of oil-in-water emulsion (occurs in applications such as fracking) was studied. The sample feed composed of vegetable oil, NaCl, water, and Pluronic F 68 as surfactant. Sample #100 was used as membranes in this experiment. During the test, pressure increased to values higher than 1000 KPa which suggests that the polyHIPE membrane act as a barrier for oil droplets. However, since the experiments were performed in dead-end configuration and resulted in such a high pressure, droplets are pushed through membrane and went through refining process to pass the small pores of polyHIPE membrane. Another experiment was performed in which sample feed containing talc, prepared as explained in Experimental section, was filtered through sample #100 as membrane. Synthesized membranes showed 99.9% rejection of particles and the permeability after 60 second was decreased to zero, which demonstrates the formation of cake and pore blockage due to the dead-end configuration. Therefore, the polyHIPE has the capability for removing suspending particles from water. The permeability for such experiment is shown in Table 4. It is expected that polyHIPE membranes have a much a better performance in the cross-flow configuration, where oil droplet will not be pushed

through pore of membrane and particles will be washed away from membrane surface (much lower pore blockage compared to dead-end configuration).

Table 4. Particle filtration permeability of synthesized membrane

	Sample No. 103
P atm (KPa)	101
P pump (KPa)	1430
Volume (ml)	20
Q (ml/sec)	0.33
Thickness(mm)	0.2
κ/l (m)	1.80×10^{-13}

4. Conclusion

The aim of this project was to study the possibility of using polyHIPEs as ultrafiltration (UF) and microfiltration (MF) membrane. In this regard, morphology, surface chemistry, mechanical properties, and filtration ability of polyHIPE porous materials were studied. The results show that polyHIPEs can be used as membranes because of high porosity (at least 74.05%), high pore connectivity, and acceptable mechanical properties. Also, in-situ functionalization was performed to improve permeability and rejection of membrane through incorporation of a hydrophilic monomer (sodium acrylate) in the water phase of HIPE prior to polymerization.

Comprehensive investigation of several formulations was performed and a polyHIPE with 85 wt% water phase which contains 5 wt% salt, and 0.5 wt% SA and 15 wt% oil phase contain 35 wt% PGPR as a surfactant, 0.25 wt% KPS as thermal initiator and 0.25 wt% HPK as photo initiator and monomer to cross-linker ratio of 4:1 was found as an optimum formulation for membrane fabrication in this work. Optical Microscopy, SEM, FT-IR, and conductometric titration were used for membrane characterization. Based on rejection test which shows 99.9% rejection of talc particle, the polyHIPE can be used as a particle filtration membrane. Significant increase in the pumping pressure upon filtration of oil

droplets also demonstrates that the polyHIPE membranes have the potential for oil droplet removal in industrial configuration which are cross-flow rather than dead-end. The results show that the permeability of polyHIPE membranes is significantly higher than commercial ones. Therefore, UF/MF membranes can successfully be produced from HIPE templating with potential to utilize different monomers for tuning membrane performance. In addition, the fabrication of polyHIPE membrane is ecofriendly since it uses water to generate pores instead of organic solvent.

As recommendation for future work, polyHIPE can be made with nanoemulsion to produce nanofiltration membranes.

5. References

- [1] R. F. Service, "Desalination freshens up," *Science* (80-.), vol. 313, no. 5790, pp. 1088–1090, Aug. 2006.
- [2] ed Sjoblom, Johan, *Emulsions and Emulsion Stability: Surfactant Science Series/61*, vol. 21. CRC Press, 2005.
- [3] K. J. Lissant and K. G. Mayhan, "A study of medium and high internal phase ratio water/polymer emulsions," *J. Colloid Interface Sci.*, vol. 42, no. 1, pp. 201–208, Jan. 1973.
- [4] E. D. Goddard, *Surfactants and interfacial phenomena*, vol. 40. 1989.
- [5] B. Y. W. D. Bancroft, "Bancroft, W. D. The Theory of Emulsification V.," *Changes*, vol. 3, no. 1904, pp. 501–519, 1913.
- [6] W. C. Griffin, "Classification of surface-active agents by 'HLB,'" *J Soc Cosmet. Chem.*, vol. 1, pp. 311–326, 1946.
- [7] I. Congress and S. Activity, "Emulsion Type . I . Physical Chemistry of," pp. 426–438, 1957.
- [8] T. F. Tadros, *Applied Surfactants: Principles and Applications*. Wiley-VCH Verlag GmbH & Co., 2005.
- [9] E. Ruckenstein and N. Churaev, "A possible hydrodynamic origin of the forces of hydrophobic attraction," *J. Colloid Interface Sci.*, vol. 147, no. 2, pp. 535–538, Dec. 1991.
- [10] J. R. Carnachan, "Emulsion-derived (PolyHIPE) foams for structural

- materials applications,” 2004.
- [11] N. R. Cameron, “High internal phase emulsion templating as a route to well-defined porous polymers,” *Polymer (Guildf.)*, vol. 46, no. 5, pp. 1439–1449, Feb. 2005.
- [12] K. . Lissant, “The geometry of high-internal-phase-ratio emulsions,” *J. Colloid Interface Sci.*, vol. 22, no. 5, pp. 462–468, Nov. 1966.
- [13] M. P. Aronson and M. F. Petko, “Highly Concentrated Water-in-Oil Emulsions: Influence of Electrolyte on Their Properties and Stability,” *J. Colloid Interface Sci.*, vol. 159, no. 1, pp. 134–149, Aug. 1993.
- [14] J. Kizling and B. Kronberg, “On the formation and stability of concentrated water-in-oil emulsions, aphrons,” *Colloids and Surfaces*, vol. 50, pp. 131–140, Jan. 1990.
- [15] H. M. Princen, “Highly concentrated emulsions. I. Cylindrical systems,” *J. Colloid Interface Sci.*, vol. 71, no. 1, pp. 55–66, 1979.
- [16] T. D. Dimitrova and F. Leal-Calderon, “Rheological properties of highly concentrated protein-stabilized emulsions,” *Adv. Colloid Interface Sci.*, vol. 108, pp. 49–61, 2004.
- [17] V. G. Babak and M.-J. Stébé, “Highly Concentrated Emulsions: Physicochemical Principles of Formulation,” *J. Dispers. Sci. Technol.*, vol. 23, no. 1–3, pp. 1–22, Jan. 2002.
- [18] I. Masalova, R. Foudazi, and A. Y. Malkin, “The rheology of highly concentrated emulsions stabilized with different surfactants,” *Colloids Surfaces A Physicochem. Eng. Asp.*, vol. 375, no. 1–3, pp. 76–86, Feb. 2011.
- [19] R. Foudazi, S. Qavi, I. Masalova, and A. Y. Malkin, “Physical chemistry of highly concentrated emulsions,” *Adv. Colloid Interface Sci.*, vol. 220, pp. 78–91, 2015.
- [20] R. Foudazi, P. Gokun, D. L. Feke, S. J. Rowan, and I. Manas-Zloczower, “Chemorheology of Poly(high internal phase emulsions),” *Macromolecules*, vol. 46, no. 13, pp. 5393–5396, Jun. 2013.
- [21] N. R. Cameron and D. C. Sherrington, *High internal phase emulsions (HIPES) — Structure, properties and use in polymer preparation*. Berlin, Heidelberg: Springer Berlin Heidelberg, 1996.
- [22] H. Zhang and A. I. Cooper, “Synthesis and applications of emulsion-templated porous materials,” *Soft Matter*, vol. 1, no. 2, pp. 107–113, 2005.
- [23] P. J. Colver and S. a F. Bon, “Cellular polymer monoliths made via

- pickering high internal phase emulsions,” *Chem. Mater.*, vol. 19, no. 13, pp. 1537–1539, 2007.
- [24] C. Zhao, E. Danish, N. R. Cameron, and R. Katakya, “Emulsion-templated porous materials (PolyHIPEs) for selective ion and molecular recognition and transport: applications in electrochemical sensing,” *J. Mater. Chem.*, vol. 17, no. 23, pp. 2446–2453, Jun. 2007.
- [25] A. M. Shakorfow, “Process intensification in the demulsification of water-in-crude oil emulsions via crossflow microfiltration through a hydrophilic polyHIPE polymer (PHP),” 2012.
- [26] I. Pulko, V. Smrekar, A. Podgornik, and P. Krajnc, “Emulsion templated open porous membranes for protein purification,” *J. Chromatogr. A*, vol. 1218, no. 17, pp. 2396–401, 2011.
- [27] M. Tebboth, A. Menner, A. Kogelbauer, and A. Bismarck, “Polymerised high internal phase emulsions for fluid separation applications,” *Curr. Opin. Chem. Eng.*, vol. 4, pp. 114–120, 2014.
- [28] P. Krajnc, N. Leber, D. Štefanec, S. Kontrec, and A. Podgornik, “Preparation and characterisation of poly(high internal phase emulsion) methacrylate monoliths and their application as separation media,” *J. Chromatogr. A*, vol. 1065, no. 1, pp. 69–73, Feb. 2005.
- [29] J. Su, J. Flanagan, Y. Hemar, and H. Singh, “Synergistic effects of polyglycerol ester of polyricinoleic acid and sodium caseinate on the stabilisation of water–oil–water emulsions,” *Food Hydrocoll.*, vol. 20, no. 2–3, pp. 261–268, 2006.
- [30] Z. Bhungara, “Polyhipe foam materials as filtration media,” *Filtr. Sep.*, vol. 32, no. 3, pp. 245–251, Mar. 1995.
- [31] V. O. Ikem, A. Menner, T. S. Horozov, and A. Bismarck, “Highly permeable macroporous polymers synthesized from pickering medium and high internal phase emulsion templates,” *Adv. Mater.*, vol. 22, no. 32, pp. 3588–92, Aug. 2010.
- [32] I. Pulko and P. Krajnc, “Open cellular reactive porous membranes from high internal phase emulsions,” *Chem. Commun. (Camb)*, no. 37, pp. 4481–3, 2008.